

# CMOS-Compatible Encapsulated Silver Bandpass Filters

Mina Rais-Zadeh, Hossein M. Lavasani, and Farrokh Ayazi

School of Electrical and Computer Engineering, Georgia Institute of Technology, Atlanta, GA, 30308, USA

**Abstract** — This paper presents the design, implementation, and characterization of low insertion loss (IL) encapsulated silver bandpass filters for radio frequency integrated circuits. The effect of the metal and the substrate loss on the performance of the filter is investigated. A polymer-encapsulated third-order elliptic filter shows an embedded insertion loss of 1.9 dB at 1.2 GHz with a bandwidth of 300 MHz.

**Index Terms** — bandpass filters, elliptic filters, micromachining, packaging, Q factor, silver.

## I. INTRODUCTION

The majority of bandpass filters used in cellular modules are currently realized using off-chip acoustic-resonant components, such as SAW and FBAR devices. Size reduction has continued to pose a challenge to system designers, as off-chip components occupy additional board area and require separate packaging. On the other hand, off-chip components must interface with integrated electronics at the board level, which introduces additional loss because of the interconnects. Integrated single chip solutions to cellular modules are therefore highly desirable.

Recent developments have resulted in high-performance micromachined passive components at gigahertz frequencies that can potentially be integrated with RF circuits [1, 2]. The availability of CMOS-compatible high-Q micromachined inductors and capacitors can help reduce the number of off-chip components while preserving the performance of the cellular modules. To this date, little effort has been made towards implementation and characterization of integrated lumped-element passive filters with micromachined components. This is mainly due to the fact that the loaded-Q values of individual on-chip inductors and capacitors have not been high enough to yield high-order bandpass filters with low insertion loss.

In this paper, we present implementation of low insertion loss bandpass elliptic filters on CMOS-grade ( $\rho = 10\text{-}20 \Omega\cdot\text{cm}$ ) silicon (Si) substrate that are fabricated and encapsulated (at the wafer level) using a CMOS-compatible process. The effect of the metal and the substrate loss on the filter performance is described and validated by fabricating several filters with different metal thicknesses on various substrates. An optimized elliptic LC filter exhibits a low insertion loss (IL) of 0.9 dB at 1.2 GHz. Wafer-level polymer encapsulation of the filters did not cause any additional loss.

## II. FABRICATION

We reported a CMOS-compatible fabrication process to implement high-performance silver passive components in [1]. The elliptic bandpass filters reported here are realized using the same fabrication process. A brief description of the process flow is as follows: the substrate is first passivated with the low-loss Avatrel polymer ( $\sim 20\mu\text{m}$  thick) to reduce the parasitics of the pads. A routing layer is evaporated and patterned. Next, a PECVD silicon dioxide dielectric layer is deposited and patterned. Thick silver is then electroplated into a high aspect-ratio photoresist mold. The loss of Si substrate is eliminated by selective etching of the Si underneath the filters from the backside, leaving behind a firmly-supported Avatrel membrane. The filters are encapsulated at wafer-level in 3 simple steps [3]. First, a thermally-decomposable sacrificial polymer (Unity) is applied and patterned. Then, the over-coat polymer (Avatrel) is spin-coated and patterned. Finally, the sacrificial polymer is thermally decomposed at  $180^\circ\text{C}$  (the highest temperature of the entire process flow). Figure 1 schematically shows the cross-section view of a resulting encapsulated filter.

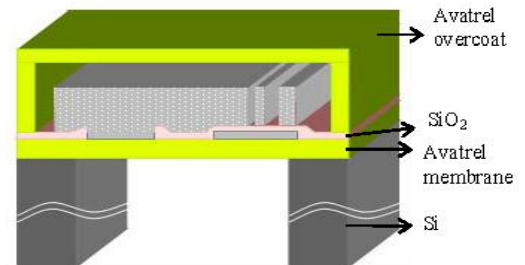


Fig. 1. Schematic view of an encapsulated filter on the polymer membrane.

## III. DESIGN AND SIMULATION

Among different LC filter configurations, elliptic filters require the fewest components with the most practical values to attain a specific filter Q. This not only makes the fabrication of such filters easier, but also minimizes the die area. In addition, elliptic filters offer the best out-of-band rejection. A drawback is the filter group delay, which is still good enough for most cellular applications. For these reasons, we have chosen the elliptic configuration for our bandpass filters. Filters are designed with the following restrictions on the component values:

- Inductor values should be between 0.6 - 10 nH for practical high-Q ( $Q > 100$ ) implementation.
- Capacitor values should not exceed 10 pF, for the same reason. The minimum value of the capacitance is defined by the parasitic capacitances and is about 0.1 pF.

With the above-mentioned specifications, an array of four non-overlapping third-order bandpass elliptic LC filters was designed between 1-2 GHz. These filters can be placed in between the antenna and higher-Q acoustic filters to improve the overall out-of-band rejection, remove their spurious modes, and provide impedance transformation. The circuit diagram of one of the elliptic filters is shown in Fig. 2.

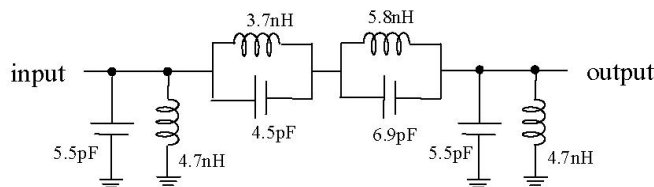
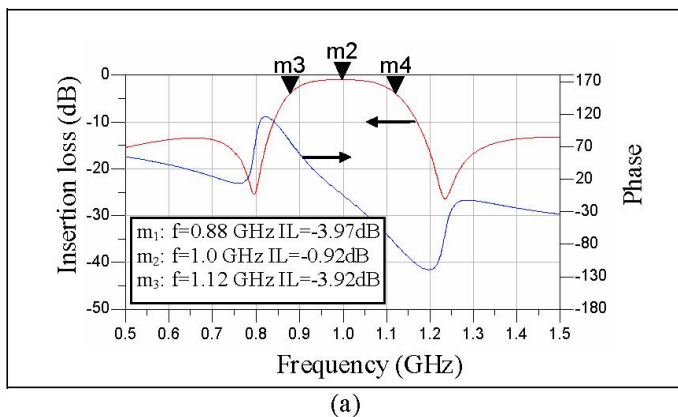


Fig. 2. Circuit diagram of the third-order bandpass elliptic filter at 1 GHz.

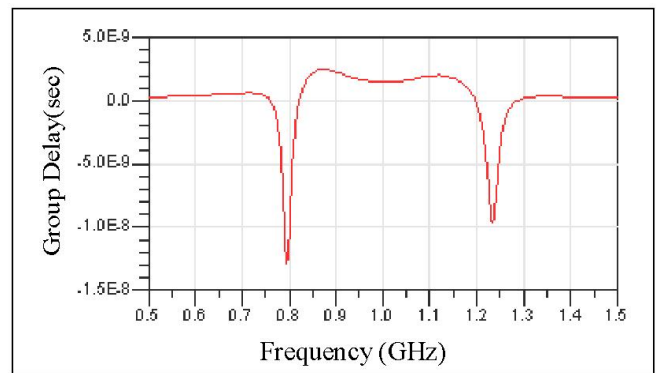
The filters are designed to have 300 MHz bandwidth with center frequencies in the range of 1.05 GHz to 1.95 GHz. Small in-band ripple is traded off for higher out-of-band rejection and reasonable values of inductors and capacitors. Initial filter design and simulation is done in Agilent hpADS tool using lumped element models for inductors and capacitors. Final optimization is performed on the filter layout in Sonnet 2.5D EM simulation tool using Sonnet thick metal model.

#### A. ADS design

The simulated frequency response of the filter at 1GHz (Filter A), when terminated to 50  $\Omega$ , is shown in Fig. 3(a). In the filter simulation, the inductor and the capacitor Qs were taken as 60 and 120, respectively. The simulated group delay of the filter is shown in Fig. 3(b).



(a)



(b)

Fig. 3. Simulated (a) frequency response and (b) group delay of Filter A at passband.

#### B. Sonnet EM simulation

The physical layout of the bandpass filters was finalized in Sonnet by optimizing the layout of the incorporated passives to get the desired frequency response for each individual LC tank, while keeping the length of the interconnects short to minimize parasitic effects. The Sonnet simulated frequency response of the filters is shown in Fig. 4.

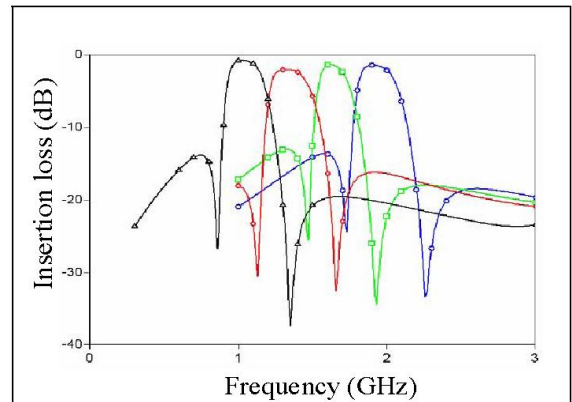


Fig. 4. Simulated frequency response of an array of four non-overlapping bandpass elliptic filters.

## IV. RESULTS AND DISCUSSION

The fabricated bandpass filters were tested using an Agilent E8364B vector network analyzer and cascade infinity GSG micro probes. The parasitics of the pads were not de-embedded from the filter frequency response.

Figure 5 compares the measured and the Sonnet simulated frequency response of Filter A. As shown in the figure, the measured frequency response is in good agreement with the EM simulation. Figure 6 shows the SEM view of the Filter A.

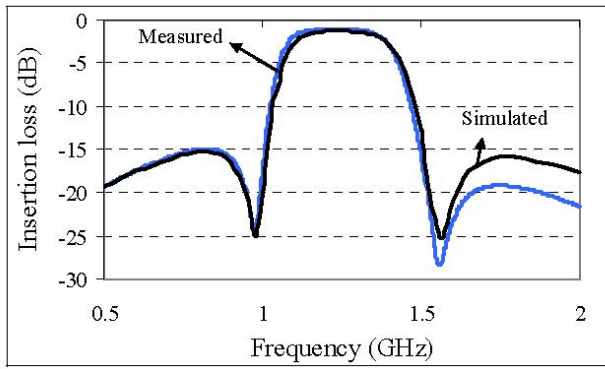


Fig. 5. Measured and simulated frequency response of Filter A at passband.

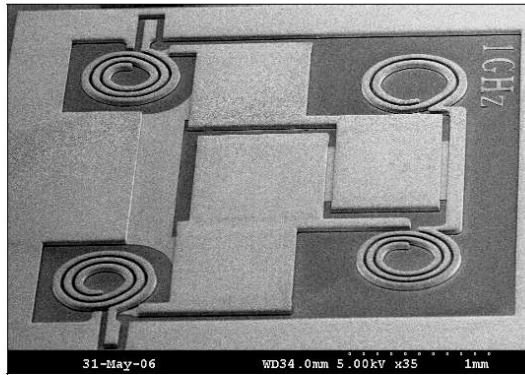


Fig. 6. SEM view of Filter A (the second metal layer is 40  $\mu\text{m}$  thick and the routing layer is 4  $\mu\text{m}$  thick).

#### A. Effect of the substrate loss

To demonstrate the effect of the substrate loss, two identical filters were fabricated on an Avatrel membrane (Si removed from the backside) and an Avatrel-passivated CMOS-grade Si substrate. The fabricated filter on Avatrel membrane exhibits a very low IL of 0.9 dB at 1.2 GHz when terminated to 50  $\Omega$ , which corresponds to a loaded inductor Q of 60 and a loaded capacitor Q of 100 at 1.2 GHz. The identical filter on Avatrel-passivated Si has an IL of 3.6 dB.

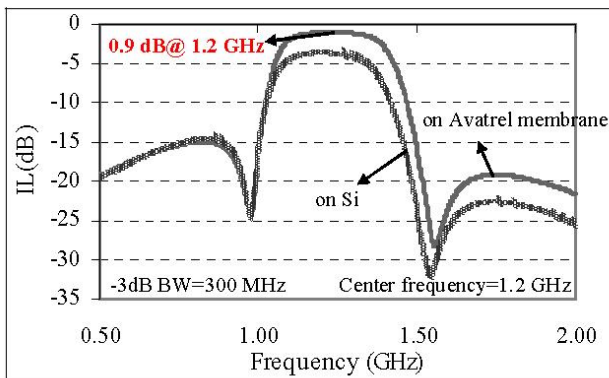


Fig. 7. Measured  $S_{21}$  of Filter A on Avatrel membrane and Avatrel-passivated Si, showing an IL of 0.9 dB on Avatrel and 3.6 dB on Avatrel-passivated CMOS-grade Si.

Figure 8 shows the frequency response of the Filter A fabricated on high-resistivity silicon substrate ( $\rho > 1 \text{ k}\Omega\cdot\text{cm}$ ). In this case, the passivation layer is only 1  $\mu\text{m}$  silicon nitride + 1  $\mu\text{m}$  silicon dioxide. Despite the passivation layer being much thinner than that of the filter shown in Fig. 7, the insertion loss is increased only by 1 dB (to 1.9 dB) at 1.2 GHz. This filter is packaged using a thermally released wafer-level polymer packaging technique and showed no degradation in IL after packaging. After 6 months, the filters were tested again and the packaged filter showed a slightly better IL ( $\sim 0.1 \text{ dB}$ ) compared to the un-packaged filter, as shown in Fig. 8.

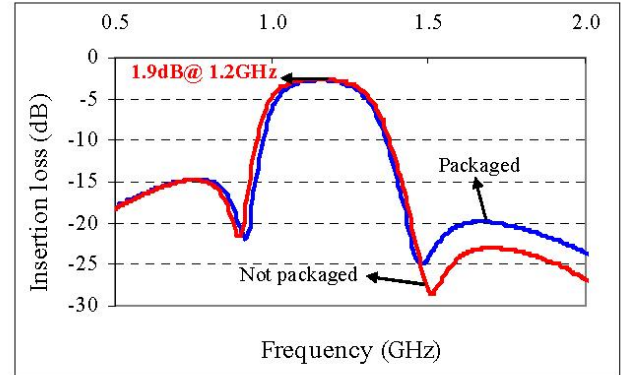


Fig. 8. Measured frequency response of Filter A fabricated on high-resistivity silicon substrate, one is packaged and the other one is not packaged.

#### B. Effect of the metal loss

Although at 1.2 GHz the skin depth of silver is much smaller than 20  $\mu\text{m}$ , since the inductor structures are coplanar, the metal loss can be improved by increasing the thickness of the metal [4, 5]. Figure 9 shows the performance of two filters fabricated on Avatrel membrane. The filter with 40  $\mu\text{m}$  thick silver exhibits 1 dB lower loss compared to the filter with 20  $\mu\text{m}$  thick silver.

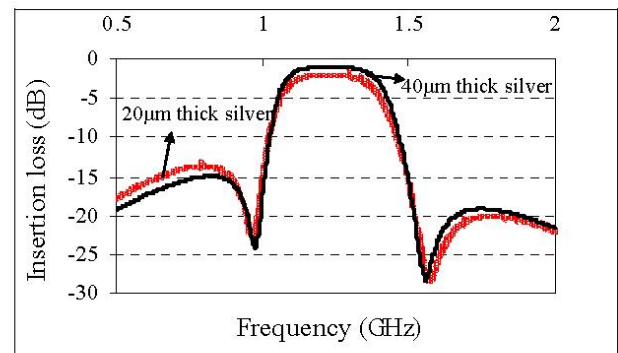


Fig. 9. Measured  $S_{21}$  of Filter A fabricated on an Avatrel membrane with two different metal thicknesses, showing an improved IL of 1 dB for the thicker silver filter.

By comparing the results of Figures 7-9 it is evident that the best performance is achieved by using 40 $\mu$ m thick silver on the Avatrel membrane.

### C. Array of filters

The array of four non-overlapping bandpass filters was fabricated on the Avatrel membrane to achieve the optimum performance. Figure 10 shows the measured frequency response of an integrated array of non-overlapping silver bandpass filters, the simulation result of which was shown in Fig. 4. The higher insertion loss, and lower out-of-band rejection of these filters compared to the simulated response is due to the thinner routing layer that was employed in this batch, which significantly added to the parasitic of the routing layer and reduced the Q of the individual passive components. Figure 11 shows the optical image of the 4" wafer. The microscopic image of a sample filter is shown in Fig. 12.

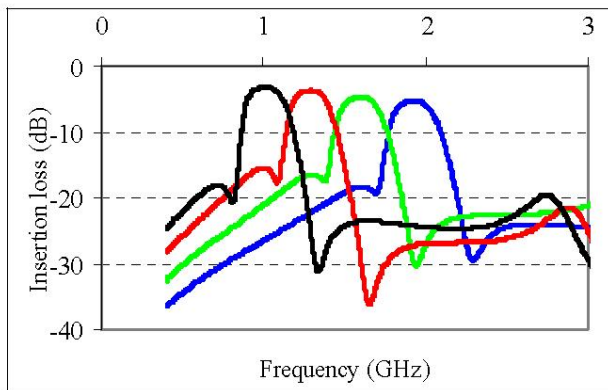


Fig. 10. Measured frequency response of an integrated array of non-overlapping bandpass filters.

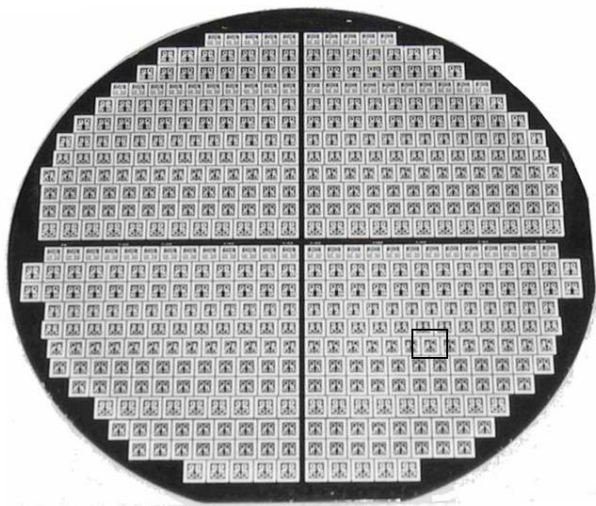


Fig. 11. Optical image of the wafer.

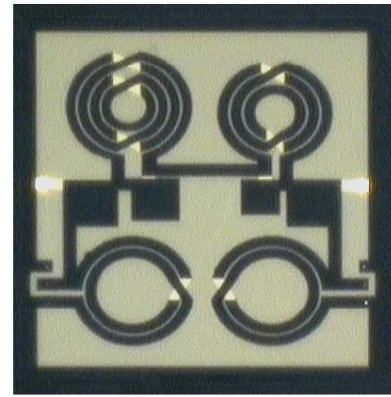


Fig. 12. Microscope image of a sample filter.

## VII. Conclusion

The design, implementation and characterization of an array of high performance encapsulated silver bandpass filters were presented. The effect of both the metal loss and the substrate loss was investigated on the performance of the filters at radio frequencies. A 40 $\mu$ m thick silver filter fabricated on Avatrel membrane showed a low insertion loss of 0.9 dB at 1.2 GHz. The polymer packaging of the filter showed no additional loss.

## ACKNOWLEDGEMENT

This work was supported by DARPA. The authors wish to acknowledge the assistance of the MiRC cleanroom staff.

## REFERENCES

- [1] M. Rais-Zadeh, P. A. Kohl, and F. Ayazi, "High-Q micromachined silver passives and filters," in *Tech. Dig. IEEE Int. Electron Device Meeting (IEDM '06)*, San Francisco, CA, Dec. 2006, pp. 727-730.
- [2] P. Carazzeti, M. A. Dubois, and N. F. de Rooij, "High performance micromachined RF planar inductors," *IEEE International Conference on Solid-state Sensors, Actuators and Microsystems (Transducers '05)*, Seoul, Korea, June 2005, pp. 1084-1087.
- [3] P. Monajemi, P. Joseph, P. Kohl, and F. Ayazi, "A low cost wafer-level MEMS packaging technology," *Proc. IEEE Micro Electro Mechanical Systems Conference (MEMS'05)*, Miami, FL, Jan. 2005, pp. 634-637.
- [4] M. Raieszadeh, P. Monajemi, S. Yoon, J. Laskar, and F. Ayazi, "High-Q integrated inductors on trenched silicon islands," *Proc. IEEE Micro Electro Mechanical Systems Conference (MEMS'05)*, Miami, FL, pp. 199-202, Jan. 2005.
- [5] Y. -S. Choi and J. -B. Yoon, "Experimental analysis of the effect of metal thickness on the quality factor in integrated spiral inductors for RF ICs," *IEEE Electron Device Letters*, vol. 25, no. 2, pp. 76-79, Feb. 2004.